Rakenteiden Mekaniikka (Journal of Structural Mechanics)
Vol. 56, No. 4, 2023, pp. 136–145
http://rakenteidenmekaniikka.journal.fi
https://doi.org/10.23998/rm.137249

A damage-plasticity model for brittle materials based on a smooth approximation of Rankine type of failure criterion

Timo Saksala[1] and Reijo Kouhia

Summary A damage-plasticity model for tensile failure analyses of brittle materials is developed. The stress states leading to a failure (inelastic strains and damage) are indicated by a rounded approximation of the Rankine criterion. This approximation is expressed in terms of the stress invariants avoiding thus the need of coordinate transformations and eigenvalue solutions required by the classical Rankine criterion. The model is formulated with the effective stress space approach, i.e., the return mapping is first performed in the global effective stress space and then the damage update is performed independently of the plasticity part. The model is consistently linearized, and, finally, some demonstrative simulations of a tensile test on a rock-like material are carried out.

Key words: Rankine failure criterion, smooth approximation, brittle materials, damage-plasticity model, finite elements

Received: 26 September 2023. Accepted: 7 December 2023. Published online: 29 December 2023.

In memory of Dr. Djebar Baroudi and Lic. Jari Laukkanen

Introduction

The Rankine, or the maximum principal stress, criterion is probably the most widely used tensile failure criterion for brittle materials. It assumes that failure occurs when the maximum principal stress at a point reaches the tensile strength of the material [1]. As it ignores the effect of the other two principal stresses, it is realistic only for brittle materials (rocks, soil, concrete, cast iron etc. [2]) in uni- or multiaxial tension.

In computational plasticity analyses of rocks and concrete, the Rankine criterion is often used as a tension cut-off surface for shear failure criteria, such as the Mohr-Coulomb

[1]Corresponding author: timo.saksala@tuni.fi

and Drucker-Prager, to mend their incorrect prediction of the tensile strength and failure modes [3–6]. These bi-surface plasticity models usually result in discontinuity of the yield direction at the intersection of the yield surfaces [4]. The return mapping in such case of corner plasticity is naturally more involved, as the return direction is not unique [4,7,8]. A way to circumvent the non-smooth intersection between the different yield surfaces is to formulate a single surface approximation, as done in [9], which presents a smooth and convex yield surface for concrete under both tension and compression. This, however, comes at the cost of more complicated mathematical expression of the yield criterion.

Another aspect of implementation is that the Rankine criterion has a simple linear form ($\sigma_1 - \sigma_\mathrm{t}$, where the first and second term are the maximum principal stress and the tensile strength, respectively) only in the principal stress space while its expression in the global stress space is nonlinear [10]. This means, on one hand, that the closed form return mapping is lost and the numerical implementation is more complicated as iteration and coordinate transformations are needed. On the other hand, the solution of the eigenvalue problem is not needed if the Rankine criterion is expressed in the Haigh-Westergaard coordinates.

In light of the discussion above, there are advantages and disadvantages in both the principal and the global stress space formulations. Despite this, the avenue pursued in this paper is to employ a single surface rounded approximation to the original Rankine cube. The properties of the approximation, based on an integer power of the trace of the modified stress tensor, are more thoroughly discussed in a companion paper [11]. Based on this criterion, which can also be expressed in terms of stress invariants, a damage-plasticity model for tensile failure of brittle materials is developed. The model development is motivated by the advantages, which overweigh the disadvantages, of using such an approximation. Namely, the approximation avoids the need to solve the eigen problem and to use the coordinate transformation, as well as has a simple tensorial form in the global stress space.

In the present model, the plasticity part of the model accounts for the inelastic strains and the damage part with a single scalar damage variable describes the degradation of strength and stiffness of a brittle material under tensile loading. The model is consistently linearized and demonstrated in representative numerical examples.

Numerical model

Plasticity model for tensile failure of brittle materials

We assume that the readers are familiar with the fundamentals of computational plasticity (if this is not the case, see [7, 10]). Thereby, we proceed to define the specific model dealt with in this paper within the small deformation framework enabling the additive decomposition of the total strain into elastic and plastic parts. A perfectly plastic behaviour, preceded by a linear elastic initial stage, is assumed for the material. Therefore, as the damage part of the model describes the degradation of the stiffness and strength, separate softening law is not needed. The plasticity model consisting of the tensile yield criterion approximating the Rankine cube augmented to include compression failure with its gradient (with respect to stress), the flow rule, and the loading-unloading conditions is then written as

$$f_n(\bar{\boldsymbol{\sigma}}) = \mathrm{tr}((\bar{\boldsymbol{\sigma}} - \alpha\mathbf{I})^n) - \beta^n \tag{1}$$

$$\frac{\partial f_n(\bar{\boldsymbol{\sigma}})}{\partial \boldsymbol{\sigma}} = n(\bar{\boldsymbol{\sigma}} - \alpha\mathbf{I})^{n-1} \tag{2}$$

$$\dot{\boldsymbol{\varepsilon}}_\mathrm{p} = \dot{\lambda}\frac{\partial f_n(\bar{\boldsymbol{\sigma}})}{\partial \boldsymbol{\sigma}} \tag{3}$$

$$f_n \leq 0,\ \dot{\lambda} \geq 0,\ f_n\dot{\lambda} = 0 \tag{4}$$

where symbol meanings are as follows: $\bar{\boldsymbol{\sigma}}$ is the effective stress tensor (see (9)); $\dot{\boldsymbol{\varepsilon}}_\mathrm{p}$ is the rate of the plastic strain $\boldsymbol{\varepsilon}_\mathrm{p}$; $\dot{\lambda}$ is the rate of the plastic multiplier λ, $\mathbf{I}$ is the second order identity tensor, and for even powers n, coefficients α and β can be expressed in terms of the uniaxial compressive strength-like parameter (σ_ca, while the material compressive strength is σ_c) and tensile strength (σ_t) as

$$\alpha = \tfrac{1}{2}(\sigma_\mathrm{t} - \sigma_\mathrm{ca}),\ \beta^n = 2\left(\tfrac{1}{2}(\sigma_\mathrm{t} - \sigma_\mathrm{ca})\right)^n + \left(\tfrac{1}{2}(\sigma_\mathrm{t} + \sigma_\mathrm{ca})\right)^n \tag{5}$$

Figure 1a illustrates the Rankine yield surface and the rounded approximation in 2D case with n = 4 and n = 6. It should be noted that the approximation approaches the Rankine yield surface when $n \to \infty$. The approximation error is further discussed in the companion paper [11]. Moreover, the elasticity parameters σ_t and σ_ca are independent of the integer power n. This can be seen in Figure 1a, where the approximations cut intersect the principal stress axes at the same values (i.e., at σ_t and σ_ac). It is also remarked that a recursion formula to express the yield criterion (1) in terms of stress tensor invariants can be proven [11] for general case n. For example, in case n = 4 the approximation has the following invariant form

$$\begin{aligned} f_4(I_1, I_2, I_3) = I_1^4 + 4I_1^2 I_2 + 2I_2^2 - 4\alpha(I_1^3 + 3I_1 I_2 + 3I_3) + \\ +6\alpha^2(I_1^2 + 2I_2) - 4\alpha^3 I_1 + 3\alpha^4 - \beta^4 \end{aligned} \tag{6}$$

where $I_1 = \mathrm{tr}(\boldsymbol{\sigma} - \alpha\mathbf{I})$, $I_2 = \frac{1}{2}(\mathrm{tr}(\boldsymbol{\sigma} - \alpha\mathbf{I})^2 - (\mathrm{tr}(\boldsymbol{\sigma} - \alpha\mathbf{I}))^2)$, and $I_3 = \det(\boldsymbol{\sigma} - \alpha\mathbf{I})$. This expression is, however, only of theoretical interest, as form (1) is substantially more economical from the computational point of view. Finally, the original Rankine criterion considered only tensile failure, but the present modification also includes the compressive strength. Clearly, when $\sigma_\mathrm{ca} = \sigma_\mathrm{t} \Rightarrow \alpha \equiv 0$, and thus the influence of the compressive strength disappears. However, there is an implementation reason to include the compressive strength described graphically in Figure 1b showing the Rankine criterion and examples of the present smooth approximation as cut-off to the Mohr-Coulomb (MC) shear criterion in 2D. When the compressive strength parameter of the approximation equals the tensile strength of the material, i.e., $\sigma_\mathrm{ca} = \sigma_\mathrm{t}$, it may happen with realistic values of material compressive strength (σ_c) and internal friction angle of the material that the approximation does not intersect the MC cone, as illustrated in Figure 1b. In such a case, the stress return mapping cannot be uniquely defined as the tensile cut-off criterion is inside the shear cone. This problem disappears when $\sigma_\mathrm{ca} > \sigma_\mathrm{t}$ and the criteria intersect, as illustrated in Figure 1b.

For brittle materials, the macrofailure plane in uniaxial tension is perpendicular to the axis of loading [2]. When modelling uniaxial tension with the plasticity approach, this means that the yield direction, representing the crack opening, should be perpendicular to the macrofailure plane, i.e., parallel to the loading axis. As the gradient of the yield surface is the yield direction in the associated plasticity, the values of the coefficients in (5) call some attention.

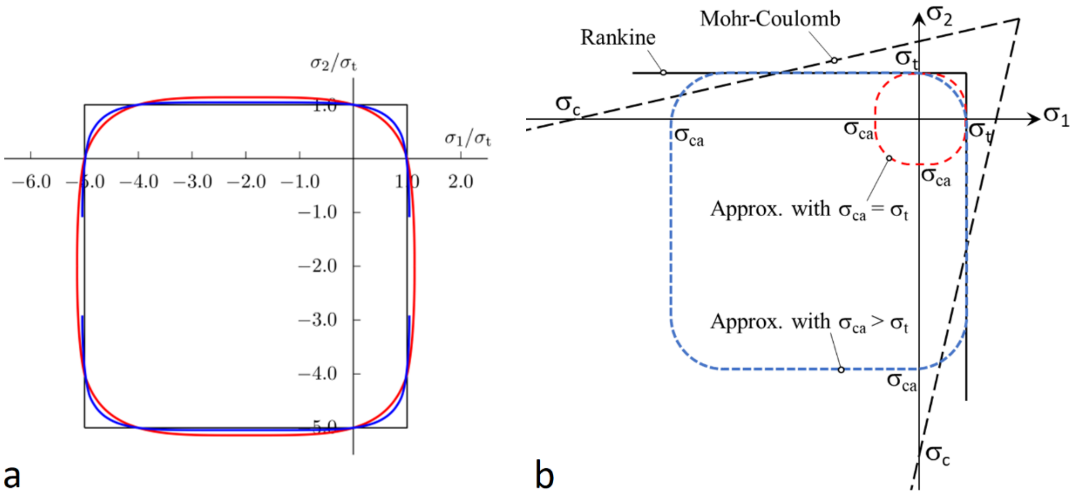

Figure 1. Rankine type failure criterion (thin black line) and its approximation in plane stress for $n = 4$ (red line) and 6 (blue line) with $\sigma_{ca} = 5\sigma_t$ (a); The Rankine failure criterion as a tensile cut off for the Mohr-Coulomb criterion and the approximation in plane case (b).

Consider uniaxial tension with $\sigma_x = \sigma_t$ and the rest of the stress components are zero. Then, with $\sigma_{ca} = 10\sigma_t$ (typical ratio for concrete and rock), Equation (5) gives $\alpha = -9/2\,\sigma_t$. Now, by Equation (2) the yield direction, in Voigt notation, becomes $n\sigma_t/2[11\ 9\ 9\ 0\ 0\ 0]^{n-1}$, which with small n, being almost hydrostatic dilatation, is not correct. The correct yield direction, having only the component in x-direction nonzero, is obtained when $\alpha = 0$, i.e., when $\sigma_{ca} = \sigma_t$ or, alternatively, when $n \to \infty$. While this is not correct for any brittle material, it can be used for geomaterials since the compressive/shear behaviour for these materials is modelled by a separate shear yield criterion, as discussed above. Therefore, we proceed with this setting.

Scalar damage model for tensile failure of brittle materials

A scalar damage model is chosen for simplicity. If the reader is unfamiliar with the concepts of damage mechanics, Ref. [2] is recommended. A scalar damage model with an exponential softening function (i.e., the integrated form of damage evolution law $\dot{\omega} = f(\omega, \boldsymbol{\varepsilon}, \boldsymbol{\varepsilon}_p, \ldots)$) driven by plastic strain, the equivalent plastic strain (ε^p_{eqvt}), the nominal-effective stress relation, and the constitutive law are written as

$$\omega_t(\varepsilon^p_{eqvt}) = g_t(\varepsilon^p_{eqvt}) = A_t(1 - \exp(-\beta_t \varepsilon^p_{eqvt})) \tag{7}$$

$$\dot{\varepsilon}^p_{eqvt} = \tfrac{1}{3}\langle \mathrm{tr}(\dot{\boldsymbol{\varepsilon}}_p)\rangle, \ \ \beta_t = \sigma_t h_e/G_{Ic} \tag{8}$$

$$\boldsymbol{\sigma} = (1 - \omega_t)\bar{\boldsymbol{\sigma}} = (1 - \omega_t)\mathbf{C}_e : (\boldsymbol{\varepsilon} - \boldsymbol{\varepsilon}_p) \tag{9}$$

where ω_t is the tensile damage variable, A_t and β_t are parameters controlling the maximum value of damage and the amount dissipation during the softening process, respectively. Parameter β_t is calibrated in (8) by the mode I fracture energy G_Ic and the characteristic length of a finite element h_e, i.e., it is element specific. Moreover, Macaulay brackets have been used in the rate form of the equivalent plastic strain in (8). This means that damage evolves mainly under tensile type of loading. Finally, $\mathbf{C}_\mathrm{e}$ is the elastic stiffness tensor. It is obvious by (9) that the unilateral conditions – stiffness recovery upon stress reversal from tension to compression – of microcracking in mode-I loading is neglected in this study.

It should also be noted that the damage model has no loading function to show which stress/strain states lead to damage evolution. This is because the damaging is driven by the plastic strain so that when there is plastic straining, there is also damaging. This is actually the nominal-effective stress space formulation by Grassl and Jirasek [5], which enables separation of the plasticity and damage computations so that, first, the return mapping is performed on the effective stress ($\bar{\boldsymbol{\sigma}}$) violating the yield criterion. Then the damage variable is updated, and the nominal stress is obtained, as indicated in Equation (9).

Linearization of the model: tangent stiffness operator

The stress integration, i.e., the return mapping algorithm, requires a consistent tangent operator to retain the quadratic convergence of the Newton-Raphson iteration. With the present method, the linearization starts with a perturbation (variation) of Equation (9):

$$\delta\boldsymbol{\sigma} = (1-\omega_\mathrm{t})\delta\bar{\boldsymbol{\sigma}} - \delta\omega_\mathrm{t}\bar{\boldsymbol{\sigma}} \tag{10}$$

where $\delta\omega_\mathrm{t}$ can be readily obtained from (7) and (8) as

$$\delta\omega_\mathrm{t} = \frac{dg_\mathrm{t}}{d\varepsilon^\mathrm{p}_\mathrm{eqvt}}\frac{\partial\varepsilon^\mathrm{p}_\mathrm{eqvt}}{\partial\boldsymbol{\varepsilon}_\mathrm{p}}:\delta\boldsymbol{\varepsilon}_\mathrm{p} = \mathbf{T}_\mathrm{d}:\delta\boldsymbol{\varepsilon}_\mathrm{p} \tag{11}$$

$$\mathbf{T}_\mathrm{d} = \tfrac{1}{3}\beta_\mathrm{t}A_\mathrm{t}\exp\left(-\beta_\mathrm{t}\varepsilon^\mathrm{p}_\mathrm{eqvt}\right)\langle\mathrm{sgn}\left(\Delta\boldsymbol{\varepsilon}_\mathrm{p}\right)\rangle\mathbf{1} \quad (\mathbf{1}_{ij} = \delta_{ij}) \tag{12}$$

where g_t is the damage function in (7), $\Delta\boldsymbol{\varepsilon}_\mathrm{p}$ is the plastic strain increment during the return mapping, and δ_{ij} is the Kronecker delta. Next, the variation of the effective stress is derived by first perturbing Equation (3), and then perturbing the constitutive equation as well as utilizing the consistency condition $\dot{f}_n = 0$:

$$\delta\boldsymbol{\varepsilon}_\mathrm{p} = \Delta\lambda\frac{\partial^2 f_n}{\partial\bar{\boldsymbol{\sigma}}^2}:\delta\bar{\boldsymbol{\sigma}} + \delta\lambda\frac{\partial f_n}{\partial\bar{\boldsymbol{\sigma}}} \tag{13}$$

$$\delta\bar{\boldsymbol{\sigma}} = \mathbf{C}_\mathrm{e}:(\delta\boldsymbol{\varepsilon} - \delta\boldsymbol{\varepsilon}_\mathrm{p}) \tag{14}$$

$$\delta\lambda = \frac{\partial f_n}{\partial\bar{\boldsymbol{\sigma}}}:\mathbf{C}_\mathrm{e}:\delta\boldsymbol{\varepsilon}/\frac{\partial f_n}{\partial\bar{\boldsymbol{\sigma}}}:\mathbf{C}_\mathrm{e}:\frac{\partial f_n}{\partial\bar{\boldsymbol{\sigma}}} \tag{15}$$

With these results in hand, the final form of the tangent operator, $\mathbf{E}_\mathrm{epd}$, is, after some tensor algebra, written as

$$\delta\boldsymbol{\sigma} = \mathbf{E}_{\mathrm{epd}} : \delta\boldsymbol{\varepsilon} \quad \text{with} \tag{16}$$

$$\mathbf{E}_{\mathrm{epd}} = (1-\omega_{\mathrm{t}})\mathbf{C}_{\mathrm{e}} - \left((1-\omega_{\mathrm{t}})\mathbf{C}_{\mathrm{e}} + (\overline{\boldsymbol{\sigma}} \otimes \mathbf{T}_{\mathrm{d}})\right) \cdot \mathbf{C}_{\mathrm{p}} \tag{17}$$

$$\mathbf{C}_{\mathrm{p}} = \left(\mathbb{I} + \Delta\lambda \frac{\partial^2 f_n}{\partial \overline{\boldsymbol{\sigma}}^2} \cdot \mathbf{C}_{\mathrm{e}}\right)^{-1} \left(\Delta\lambda \frac{\partial^2 f_n}{\partial \overline{\boldsymbol{\sigma}}^2} \cdot \mathbf{C}_{\mathrm{e}} + \frac{\frac{\partial f_n}{\partial \overline{\sigma}} \otimes \frac{\partial f_n}{\partial \overline{\sigma}} : \mathbf{C}_{\mathrm{e}}}{\frac{\partial f_n}{\partial \overline{\sigma}} : \mathbf{C}_{\mathrm{e}} : \frac{\partial f_n}{\partial \overline{\sigma}}}\right) \tag{18}$$

where $\mathbb{I}$ is the fourth order identity tensor. The second derivatives, or the Hessian, of the yield criterion in the case $n = 4$, used in the numerical examples, are obtained in straightforward manner:

$$\left(\frac{\partial^2 f_4(\overline{\boldsymbol{\sigma}})}{\partial \overline{\boldsymbol{\sigma}}^2}\right)_{abcd} = 4(\delta_{ac}\xi_{bd}^2 + \xi_{ac}\xi_{bd} + \xi_{ac}^2\delta_{bd}), \; \xi_{ij} = \bar{\sigma}_{ij} - \alpha\delta_{ij} \tag{19}$$

Before presenting the numerical simulations, it should be noted that the model has no regularization, i.e., it belongs to the class of classical strain (or damage) softening models. Consequently, the predicted plastic deformation localizes, upon mesh refinement, to a zone with a width of single element, as the underlying partial differential equation loses its ellipticity (or hyperbolicity in dynamics).

Numerical examples

Single element example: the model prediction in cyclic loading

The model behavior is demonstrated first at a material point level with a single element mesh. The general yield criterion is implemented in case $n = 4$.

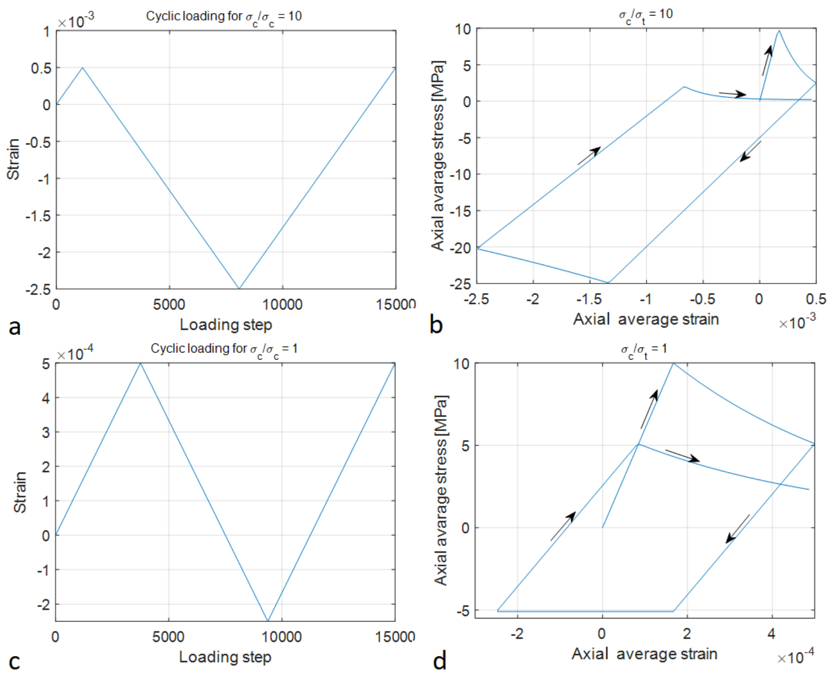

Figure 2. Model response in cyclic loading: Imposed strain (a) and model response (b) when $\sigma_{\mathrm{ca}} = 10\sigma_{\mathrm{t}}$; Imposed strain (c) and model response (d) when $\sigma_{\mathrm{ca}} = \sigma_{\mathrm{t}}$.

A standard displacement driven load reversal loading is imposed upon one edge of the model while the opposite edge is simply supported. The global system of discretized system of balance equations is solved with the Newton-Raphson iteration in a fully standard manner with a Matlab implementation. Material and model parameters used are as follows: Young's modulus E = 60 GPa; Poisson's ratio ν = 0.25; σ_t = 10 MPa; G_{Ic} = 20 J/m^2; A_t = 0.98. The results of this simulation for two different rations of the strength ration are shown in Figure 2. The average stress and strain, used to represent the results in all the simulations below, are obtained, respectively, by dividing the sum of the internal forces and the displacement at the top edge by the cross-sectional area of the model for stress and by the height of the model for strain.

The model response starts with a tension cycle, which leads to substantial yielding and softening by damage with both values of σ_{ca}. As no stiffness recovery scheme was implemented, the consequent compressive cycle takes place with the degraded stiffness due to which the correct compressive strength is not reached. More specifically, the maximum compressive stress reached, with the loading program in Figure 2a (σ_{ca} = $10\sigma_t$), is 25 MPa. In this case, the compressive cycle clearly results in further damage evolution (Figure 2b), while in case $\sigma_{ca} = \sigma_t$ (Figure 2d) the damage evolution is so slow that the response is practically perfectly (ideally) plastic.

2D simulations demonstrating approximation parameter effects

Representative 2D simulations using bilinear quadrilateral elements are carried out here. The model behavior with different values of the approximation parameters is demonstrated. The material parameters are: Young's modulus E = 60 GPa; Poisson's ratio ν = 0.25; σ_t = 10 MPa; G_{Ic} = 100 J/m^2; A_t = 0.98.

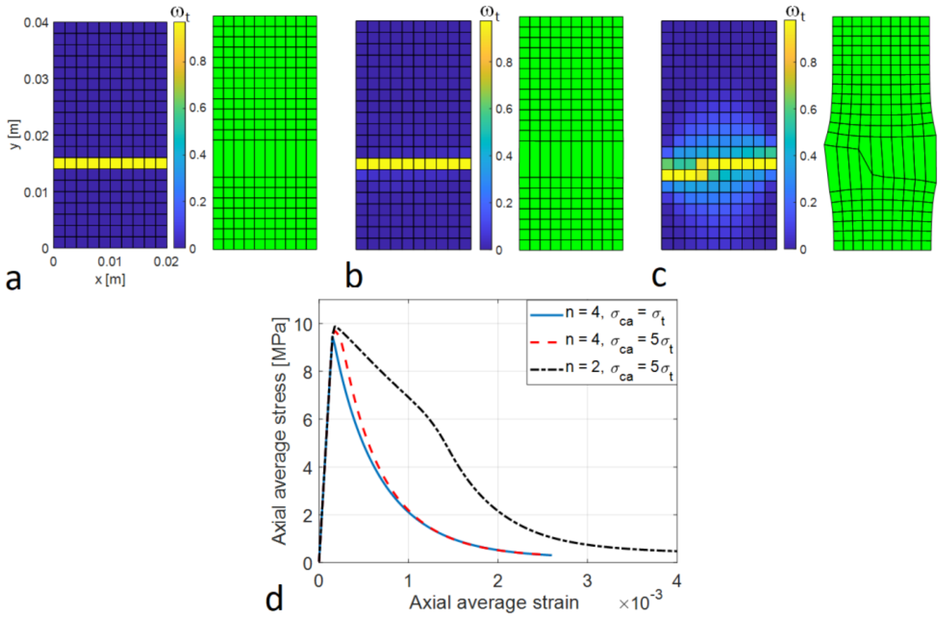

Figure 3. 2D simulation results for uniaxial tension test: Failure modes in terms of tensile damage and magnified deformed meshes when n = 4, $\sigma_{ca} = \sigma_t$ (a); n = 4, $\sigma_{ca} = 5\sigma_t$ (b); n = 2, $\sigma_{ca} = 5\sigma_t$ (c); Corresponding average stress-strain curves (c).

In order to trigger the localization naturally, the tensile strength of each element is randomly perturbed by 10 %. Figure 3 shows the simulation results for uniaxial tension for cases $n = 4$, $\sigma_{\mathrm{ca}} = 5\sigma_{\mathrm{t}}$ and $\sigma_{\mathrm{ca}} = \sigma_{\mathrm{t}}$ as well as for $n = 2$, $\sigma_{\mathrm{ca}} = 5\sigma_{\mathrm{t}}$.

When $n = 4$, the same transverse splitting mode is predicted in for both tested values of σ_{ca}, as observed in Figure 3a and b. Moreover, the corresponding average stress-strain curves in Figure 3d are quite similar. In contrast, the case $n = 2$, $\sigma_{\mathrm{ca}} = 5\sigma_{\mathrm{t}}$ deviates substantially from these due to the wrong yield direction, as discussed above. Figure 3c demonstrates that the failure mode in this case involves bulging (exaggerated here) of the mesh due the hydrostatic plastic strain.

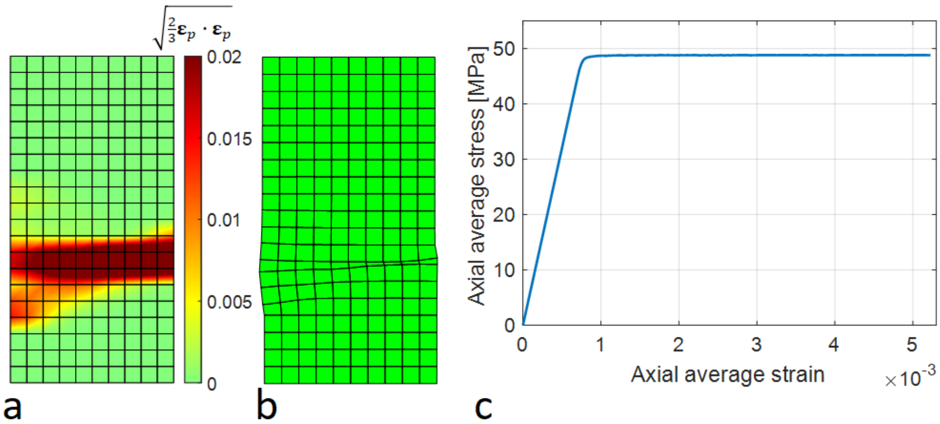

Figure 4. 2D simulation results for uniaxial compression test: Failure modes in terms of equivalent plastic strain (a) and magnified deformed meshes (b) when $n = 4$, $\sigma_{\mathrm{ca}} = 5\sigma_{\mathrm{t}}$; Corresponding average stress-strain curve (c).

The final 2D simulation demonstrates the model behavior in uniaxial compression when $n = 4$ and $\sigma_{\mathrm{ca}} = 5\sigma_{\mathrm{t}}$. As the damage model is meant for tensile damage, see Equation (8), the damage evolution is negligible and the model behavior is thus ideally plastic, as attested in Figure 4c. The failure mode predicted with this model in uniaxial compression, shown in Figure 4a in terms of equivalent plastic strain, is wrong.

3D uniaxial tension test on a laboratory size sample

Uniaxial tension test is once more carried out in full 3D case. The mesh made of 4475 trilinear hexahedral elements is used. Case $\sigma_{\mathrm{ca}} = \sigma_{\mathrm{t}}$ for the approximation is applied, while the material parameters set as in the 2D simulations above. Again, to trigger the localization naturally, the tensile strength of each element is randomly perturbed by 10 %. The simulation results for three different realization of this random strength scheme are shown in Figure 5.

The predicted failure modes include all the basic types observed in experiments: The double (conjugate) crack system (Simu1), the single macrocrack at the support (Simu2), and the single macrocrack at the weakest cross section of the sample (Simu3). The corresponding average stress-strain curves are almost identical for the cases with a single crack but more ductile for the sample failed with the conjugate crack system. This is due the fact that more energy is dissipated in this mode.

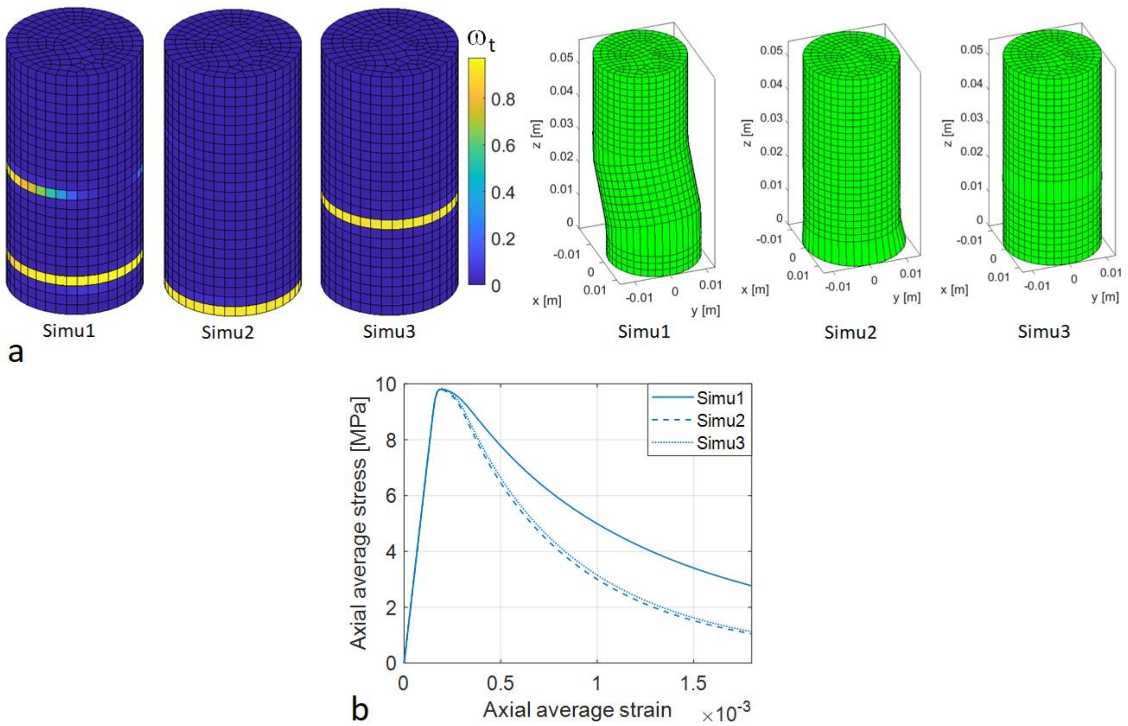

Figure 5. 3D simulation results for uniaxial tension test: Failure modes in terms of tensile damage and magnified deformed meshes (a); Corresponding average stress-strain curves (b).

Conclusions

A damage-plasticity model for brittle materials in tension based on a rounded (smooth) approximation of the Rankine criterion was presented. The rounded approximation, based on the trace of the *n*th power of the modified stress tensor, is written in terms of stress invariants so that it can be written in global stress space. It therefore circumvents the need to use coordinate transformation formulae and the solution of the eigenvalue problem, which both are required by the classical Rankine criterion. However, this comes at the cost of nonlinear, yet fairly simple, mathematical form and the loss of the closed form return mapping. Moreover, the approximation is rounded so that the flow direction in uniaxial tension is not correct with small values of n.

Despite these shortcomings, it was shown in this paper that a reasonable damage-plasticity formulation based on this yield criterion is feasible, especially when the damage and plasticity parts are separated by the effective stress space formulation. The resulting model, using the approximation with $n = 4$, correctly predicts the failure modes of rocks and concrete. Therefore, it could also serve as the tensile cut-off in a more versatile models including the compressive/shear failure description.

Acknowledgements

Research Council of Finland is gratefully acknowledged by funding this work (project ConSus – Towards sustainable carbon free concrete construction).

References

[1] W. Rankine. On the stability of loose earth. *Philosophical Transactions of the Royal Society of London*, 1857; 47.

[2] D. Krajcinovic. *Damage mechanics*. Elsevier, Amsterdam, 1996.

[3] J. Clausen. *Efficient Non-Linear Finite Element Implementation of Elasto-Plasticity for Geotechnical Problems*, PhD Thesis, Aalborg University, Denmark, 2007.

[4] T. Saksala. Damage-viscoplastic consistency model with a parabolic cap for rocks with brittle and ductile behaviour under low-velocity impact loading. *International Journal for Numerical and Analytical Methods in Geomechanics*, 34:1362–1386, 2010. https://doi.org/10.1002/nag.868

[5] P. Grassl and M. Jirásek. Damage-Plastic model for concrete failure. *International Journal of Solids and Structures*, 43:7166–7196, 2006. https://doi.org/10.1016/j.ijsolstr.2006.06.032

[6] P. Feenstra, R. De Borst. A composite plasticity model for concrete, *International Journal of Solids and Structures*, 33(5):707–30, 1996. https://doi.org/10.1016/0020-7683(95)00060-N

[7] J.C. Simo, T.J.R. Hughes. Computational Inelasticity, Springer, 1998.

[8] W.T. Koiter. Stress–strain relations, uniqueness and variational theorems for elastic–plastic materials with a singular yield surface, *Quarterly of Applied Mathematics*, 11:350–354, 1953.

[9] M. Francois. A new yield criterion for the concrete materials. *Comptes Rendus de l Académie des Sciences – Series IIB Mechanics-Physics-Chemistry-Astronomy*, 336, 5, 417–421, 2008. https://doi.org/10.48550/arXiv.1002.0856

[10] W.H. Chen and D.J. Han. *Plasticity for Structural Engineers*. Springer, 1988.

[11] R. Kouhia and T. Saksala. A recursion formula for the integer power of a symmetric second-order tensor and its application to computational plasticity. *Rakenteiden Mekaniikka (Journal of Structural Mechanics)*, 56(4):127–135, 2023. https://doi.org/10.23998/rm.137537

Timo Saksala, Reijo Kouhia
Structural mechanics, BEN, Tampere University
P.O. Box 600, FI-33101 Tampere
timo.saksala@tuni.fi, reijo.kouhia@tuni.fi